Biotechnology Reports 12 (2016) 6–12

Contents lists available at ScienceDirect

Biotechnology Reports

journal homepage: www.elsevier.com/locate/btre

Evaluation of methods for pore generation and their influence on physio-chemical properties of a protein based hydrogel

Nicholas Bodenberger, Dennis Kubiczek, Irina Abrosimova, Annika Scharm, Franziska Kipper, Paul Walther, Frank Rosenau*

Center for Peptide Pharmaceuticals, Faculty of Natural Science, Ulm University, Germany

ARTICLE INFO

Article history:
Received 12 August 2016
Accepted 8 September 2016
Available online 9 September 2016

Keywords:
Hydrogel properties
Pore size
Biopolymers
Degradation
Cell culture

ABSTRACT

Different methods to create and manipulate pore sizes in hydrogel fabrication are available, but systematic studies are normally conducted with hydrogels made of synthetic chemical compounds as backbones. In this study, a hydrogel made of natural and abundant protein in combination with different, well-available techniques was used to produce different architectures within the hydrogel matrix. Pore sizes and distribution are compared and resulting hydrogel properties like swelling ratio, resistance towards external stimuli and enzymatic degradation were investigated. Porous hydrogels were functionalized and two cancer cell lines were successfully adhered onto the material. With simple methods, pores with a radius between 10 and 80 μm and channels of 25 μm radius with a length of several hundreds of μm could be created and analyzed with laser scanning confocal microscopy and electron microscopy respectively. Furthermore, the influence of different methods on swelling ratio, enzymatic degradation and pH and temperature resistance was observed.

1. Introduction

Hydrogels are insoluble networks that can maintain huge amounts of water while keeping their insoluble form and structure [1]. Because those materials can serve as an excellent growth substrate for cells many approaches have been made to produce artificial networks for 3D cell growth in order to trigger and alter cellular behavior within those structures [2–4]. This is not only important because it represents a more realistic environment for cells than standard 2D approaches, but it also offers an enormous amount of new possibilities for the growth of cells, especially for stem cells and tumor models [5]. Numerous types of materials have a variety of properties, especially pore sizes fluctuates strongly depending on the matrix. For cell culture or tissue engineering applications, certain pore sizes in the material are crucial for sufficient oxygen transport throughout the matrix, the removal of toxic compounds and the supply of enough space for cellular outgrowth [6]. The properties and hence pore sizes of the novel materials and play a tremendous role concerning the cell type which should be cultivated and the application, with differences for each intended use: neovascularization, skin or bone regeneration and growth of special cell types like stem cells, hepatocytes or fibroblasts [7–9]. Furthermore, materials stability to environmental parameters is crucial for the use of hydrogels in complex environments like the human body which is strongly influenced by and correlates with the pore size and distribution of pores within matrices [9,10].

In recent years, extensive studies have been conducted on 3D structures of hydrogels consisting of artificial precursors [11], which are often outstanding due to their high mechanical and chemical stability and their ability to be modified to generate pores of desired sizes. Proteins, on the other hand, offer a great potential for hydrogel applications as they consist of well-defined and characterized structures which are tunable in every possible way to produce highly specific, innovative materials. In this study, a protein based hydrogels was developed and the feasibility of different, well available strategies for the production of macro porous scaffolds for protein hydrogels and the properties of the resulting protein networks were compared. Furthermore, the feasibility for those materials in cell culture are evaluated.

A huge variety of techniques is available for tuning the 3D structures of hydrogel materials, ranging from rather simple approaches to sophisticated, new techniques from all different fields of material science. A popular technique is electrospinning to produce specific structures which can be controlled within a certain range [12]. Charged threads are formed with the help of a

* Corresponding author.
E-mail address: Frank.rosenau@uni-ulm.de (F. Rosenau).

http://dx.doi.org/10.1016/j.btre.2016.09.001

strong electric field from a polymer solution and solidification takes place when the polymer is drawn from the solution, resulting in threads in the range of nm up to μm [12]. Further techniques like soft lithography, photolithography, hydrodynamic focusing, electro-spraying and bio-printing have a high potential to properly tune the exact size of the hydrogels pores [8,9], their structures and their distribution within the matrix. However, most techniques have one major drawback: they need special equipment, are often very expensive in production or limited to a certain size, require expert knowledge in different fields and often are not applicable for protein based materials. Additionally, many of the needed chemicals or procedures used are not cell compatible [13].

On the other hand, there are several simple and robust methods which do not require special equipment, can be used in any lab at any time and are very robust and easy to reproduce. One major system is solvent casting, where particles of certain, well-controlled size are homogeneously distributed into a solution prior to solidification [13]. Salt is the most widely used material, due to its good availability at low costs. Apart from salt, affordable materials like sugar, gelatin, paraffin or chalk are good substitutes due to the potential to be eliminated from the polymer by heat, dilution or pH switches [14,15]. Another important physical approach to form pores is freeze drying, where ice crystals are formed in the matrix upon freezing of the material [16]. By drying the material in vacuum, water is sublimated leaving pores in the zones which were previously occupied by ice crystals. In gas foaming, a polymer solution is saturated with gas which is later released from the material. Sodium bicarbonate can be used to produce gas in solution which creates porous structures in the hydrogel [1].

Here, we investigate the feasibility of freeze-drying, particle-leaching and gradient freezing to control size and distribution of pores within a protein hydrogel [17]. All methods are applicable in every standard lab with cheap and well obtainable chemicals (NaCl, $CaCO_3$, liquid nitrogen, dry ice) and without special equipment. Furthermore, swelling ratio, proteolytic degradation and pH and temperature stability over a broad range were investigated to detect the influence of preparation methods on protein network properties. Finally, hydrogels were modified with a cell-adhesive peptide to investigate its feasibility in cell culture with two different cell lines.

2. Materials and methods

Bovine Serum Albumin (BSA) and Tetrakis (hydroxymethyl) phosphonium chloride (THPC) were purchased from Sigma-Aldrich (St. Louis, Missouri, USA), dilutions were stored at RT. NaCl and $CaCO_3$ were obtained from Carl Roth (Carl Roth GmbH und Co. KG, Karlsruhe, Germany), Phosphate Buffered Saline was purchased from life technologies (Carlsbad, California, USA). Rhodamine-phalloidine was purchased from Thermo Fisher Scientific (Waltham, Massachusetts, USA).

Hydrogels were prepared by mixing 100 μl of a 20% (w/v) solution of BSA with the same volume of THPC to afford a 1:1 ratio of reactive amine to hydroxy groups and polymerized in an open 96 well plate at RT within minutes.

To generate pores via freeze-drying, protein hydrogels were transferred into Eppendorf-Tubes and lyophilized (FreezeDryer Epsilon 1-6D, Christ, Osterode am Harz, Germany) over night at −85 °C and 0.05 mbar.

For particle leaching, gels were polymerized in the presence of NaCl and $CaCO_3$ (Carl Roth GmbH und Co. KG, Karlsruhe, Germany), respectively. Particles were added to hydrogels right after mixing of protein with THPC, before polymerization could take place. NaCl and $CaCO_3$ were added until a saturation effect could be observed. Half of NaCl and $CaCO_3$ crystals were grinded to reduce salt crystal size, half was left untreated. Solidification took place within minutes, leading to an even distribution of crystals in the hydrogel matrix. Afterwards, polymerized hydrogels were transferred to 5 ml of H_20 (pH 7.4 for NaCl and 6.5 for $CaCO_3$) to dilute and remove salt crystals and obtain porous hydrogels.

For gradient freezing, 200 μl hydrogels were polymerized as described above and placed on a block of dry ice at 37° RT, leading to specific site-directed freezing and channel formation within hydrogel.

After pore generation in the matrix, gels were left at room temperature for 24 h to evaporate water to get dried gels for further use. The swelling ratio for different drying methods was determined by transferring dried gels into 5 ml PBS, pH 7.4 at RT. Swelling ratio was determined by the following equation as soon as swelling equilibrium was reached:

$$\text{Swelling ratio} = \frac{Ws - Wd}{Wd}$$

Where Ws is the wet weight of the gel and Wd the weight of the dried gel.

Thermal and pH resistance were determined by bringing untreated or porous gels (200 μl) to a swelling equilibrium by immersing gels in PBS. Afterwards, hydrogels were transferred to 5 ml solution at intended pH or temperature (pH 2, 7.4, 10 and temperatures of 37 °C and 80 °C). Weight was determined at fixed time points over 7 days to determine residual weight. All experiments were performed in triplicate.

In vitro degradation was determined for all modified hydrogels and compared to unmodified ones. Gels were brought to a swelling equilibration and immersed in enzyme solution of 300 Units trypsin and pepsin at pH 7.4 and 2 respectively. Hydrogels were removed from the solution, dried with a highly absorbent paper and weighted every hour over a period of 12 h to determine residual weight. All experiments were performed in triplicate.

In order to visualize three-dimensional structures of the hydrogel, hydrogels were co-polymerized with the fluorescent dye rhodamine B (0.05 mg/ml (w/v)) and treated as described earlier with different freezing or leaching techniques. Gels were observed with a Zeiss Confocal 248 Microscope (Carl Zeiss Ag, Oberkochen, Germany) with Zen software (Zen 2012 Sp1, 250 black edition, Version 8,1,0,484) at an excitation wavelength of 561 nm to reveal 3D structures. Different regions were cut to reveal pore distribution in the gel, and distribution and size of the pores within the matrix were analyzed using the GSA image analyzer software (GSA Image Analyzer, GSA, Version 419 3.8.7).

Peptide synthesis. A microwave synthesizer (CEM Cooperation, Matthews, NC, USA) with a standard fmoc solid phase was used. The fmoc protecting group was removed with 20% (v/v) piperidine in DMF and amino acid were added in 0.2 molar equivalent to the reactor, followed by 0.5 molar equivalent HBTU and 2 molar equivalent DIEA and repeated for all amino acids followed by subsequent deprotection. The peptide was cleaved in 95% (v/v) trifluoroacetic acid (TFA), 2.5% (v/v) triisopropylsilane (TIS), and 2.5% (v/v) H_2O for one hour, precipitated and washed with cold diethyl ether followed by vacuum drying.

Peptide purification. The peptide was purified via reverse phase preparative high performance chromatography in an acetonitrile/water gradient under acidic conditions on a Phenomenex C18 Luna column (5 mm pore size, 100 Å particle size, 250/21.2 mm).To determine the peptide mass, a liquid chromatography mass spectrometry approach was used. Finally, the peptide was freeze-dried (Labconco, Kansas City, MO, USA) and stored at −20 °C.

Cryo-scanning electron microscopy. Hydrogels were mixed with 30% isopropanol over night during freezing procedure. Samples were transferred into two low mass aluminum planchettes and high pressure frozen (Engineering Office M. Wohlwend

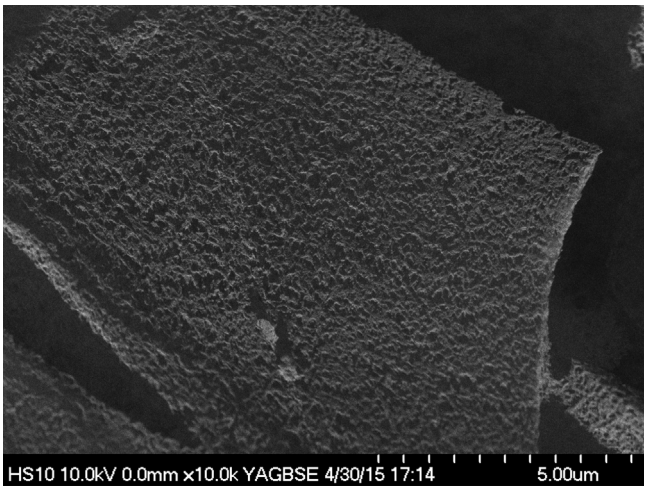

Fig. 1. Cryo scanning electron microscopy of untreated BSA Hydrogel at 10,000× (scale bar 5 μm) which was frozen under high pressure to maintain its native form.

GmbH, Sennwald, Switzerland) to maintain the native structure of the gel. Under liquid nitrogen, samples were cut to produce fractures in the gel and inserted into a freeze etching device BAF 300 (Bal-Tec, Principality of Lichtenstein) and dried at −90 °C for 30 min, followed by coating with a 3 mm platinum layer followed by subsequent analyzed with a cryo-stage Gatan 626 (Gatan-Inc., Pleasanton, California, USA). Samples were imaged at a temperature of −100 °C at an accelerating voltage of 10 kV.

Confocal microscopy of cells. Hydrogels were polymerized as described earlier in the presence of the RGD peptide in 8 well ibidi μ-slide and $2*10^5$ cells were seeded onto the hydrogel. After 24 h of adhesion, cells were fixed in 3.7% formaldehyde, washed with PBS and stained with 5 μl of 300U rhodamine-phalloidin in 200 μl PBS. Cells structures and cell adhesion were observed with confocal laser scanning microscopy at 561 nm with a Zeiss laser scanning microscope (Carl Zeiss Ag, Oberkochen, Germany).

3. Results and discussion

Protein hydrogels have gained considerable potential for biotechnological applications and are used in many different fields [5,18–20]. In most applications, the production of hydrogels with well-defined macro porous structures is desirable simultaneously maintaining the overall stability of the resulting 3D structures [21]. Here, we present a protein hydrogel which can be manipulated with diverse, simple methods to produce hydrogels with different architectures and compare the resulting materials concerning stability, swelling ratio, resistance to external stimuli and proteolytic resistance. Furthermore, the possibility to functionalize hydrogels with a cell adhesive peptide was investigated and the cellular growth of two cancer cell lines on the hydrogel was observed.

One major problem in observing hydrogel architectures with electron microscopy is the freezing procedure. The used freezing procedure has a tremendous effect on pore sizes and pore distribution in the material. To overcome this limitation, we used a high pressure freezing approach to maintain the native structure of the material as good as possible [22]. For further structural analyses, confocal laser scanning microscopy was used which was possible due to extended pore sizes in the hydrogels. This method can be applied without additional freezing of the sample, which guarantees the preservation of the materials native structure. Electron microscopic analyzes revealed pore sizes in the unmodified hydrogel in the range of several nm up to approx. 200 nm (Fig. 1). This structure introduces a high stability into the material and enables the diffusion of small molecules, but pores in the nm range are too small for most cell culture applications, e.g. ingrowth of axons into the template [23]. To change the structure of the material, gels were treated with a freeze-drying method. Extended slow ice crystal formation leads to replacement of gel structures with ice crystals which sublime upon drying at low temperature, while being gentle enough to create a porous network with intact, interconnected pores. We found the freezing temperature to have tremendous influence on gel structures: a shift from minus 20 °C to minus 196 °C – accompanied by a faster freezing – decreased the

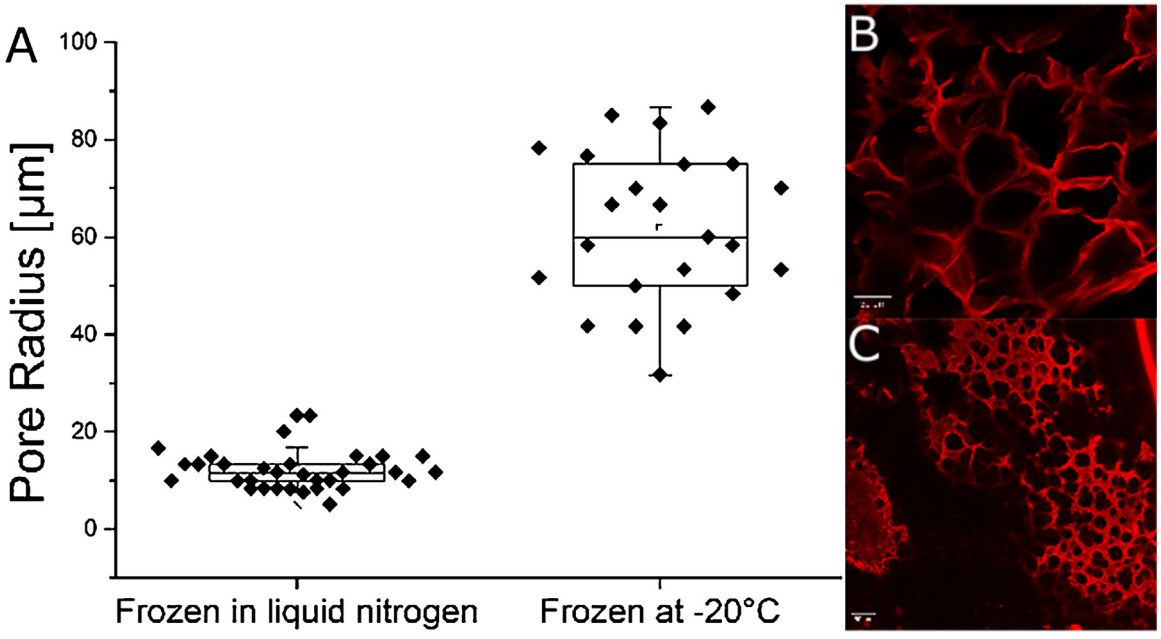

Fig. 2. Influence of pore formation and pore size for a freeze-drying approach with protein based hydrogels frozen at different temperatures. (A) Size and distribution of pores within the protein hydrogels matrix for hydrogels frozen in liquid nitrogen and at −20 °C (B)(C) Hydrogels were frozen and in liquid nitrogen (B) and at −20 °C (C) followed by subsequent freeze-drying, stained with rhodamine B and investigated via confocal laser scanning microscopy. Scale bar 50 μm.

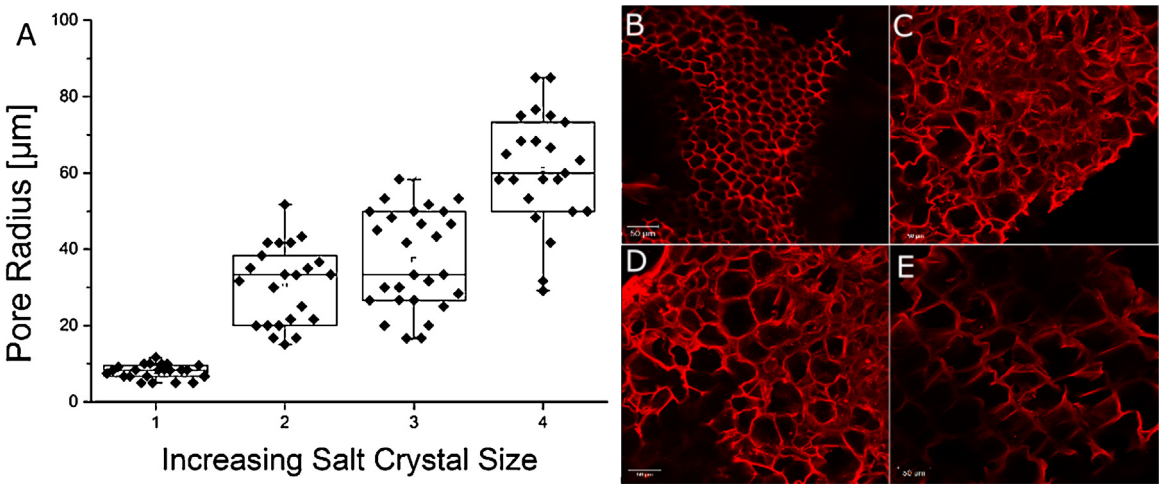

Fig. 3. Size and distribution of pores in protein hydrogels treated with a salt-leaching procedure. (A) Size distribution of pores within the protein hydrogels matrix. The used NaCl crystals were grinded with a pestle and mortar for a specific times: (B) 10 min. (C) 2 min. (D) 1 min. (E) not grinded. Protein hydrogels were stained with rhodamine B and investigated via confocal laser scanning microscopy. Scale bar 50 µm.

average pore size from up to 90 µm to only 10 µm in radius (Fig. 2). We suggest the reduced heat conduction in air compared to liquid nitrogen to further increase freezing time and thus resulting pore sizes. With this technique the biggest pores could be achieved. An alternative technique which does not require special equipment or chemicals is particle leaching. Solid particles are incorporated into the material prior to polymerization and later eluted by changing conditions [15]. To study the influence of used particle, two different chemicals were used, NaCl and $CaCO_3$. Both were added prior to solidification and later removed by increasing water volume for NaCl and acidification for $CaCO_3$ respectively. Furthermore, both particles were grinded to determine the correlation between particle sizes on pore formation. Laser scanning confocal microscopy revealed adjustable pore sizes depending on the extent of grinding. For untreated salt crystals, pore sizes of about 50 up to 90 µm radius could be created (Fig. 3). Furthermore, salt crystals which were pesteled for 1, 2 and 10 min were used and different, significantly smaller pores could be created. Especially for well-pesteled salt crystals (10 min), very small pores of about 10 µm with a very narrow distribution in size were observed (Fig. 3). For $CaCO_3$, small pores with an average size between 10 and 20 µm were produced, whereas there was no difference between pesteled and untreated $CaCO_3$, leading to the conclusion that standard $CaCO_3$ particles are already too small to be further decreased in size by standard grinding (Fig. 4). Yannas et al. [10] concluded in their study about dermal skin repair that the optimal range for this application would be pores with a radius of 10–62.5 µm, and Klawitter et al. concluded in a comprehensive study about pore sizes for cell growth of cells into a ceramic material intended for internal use to be optimal above 25 µm and below 100 µm radius and concluded the optimal size for fibroblast ingrowth to be 2.5–7.5 µm and for osteoid ingrowth to be 20–50 µm radius [24]. It

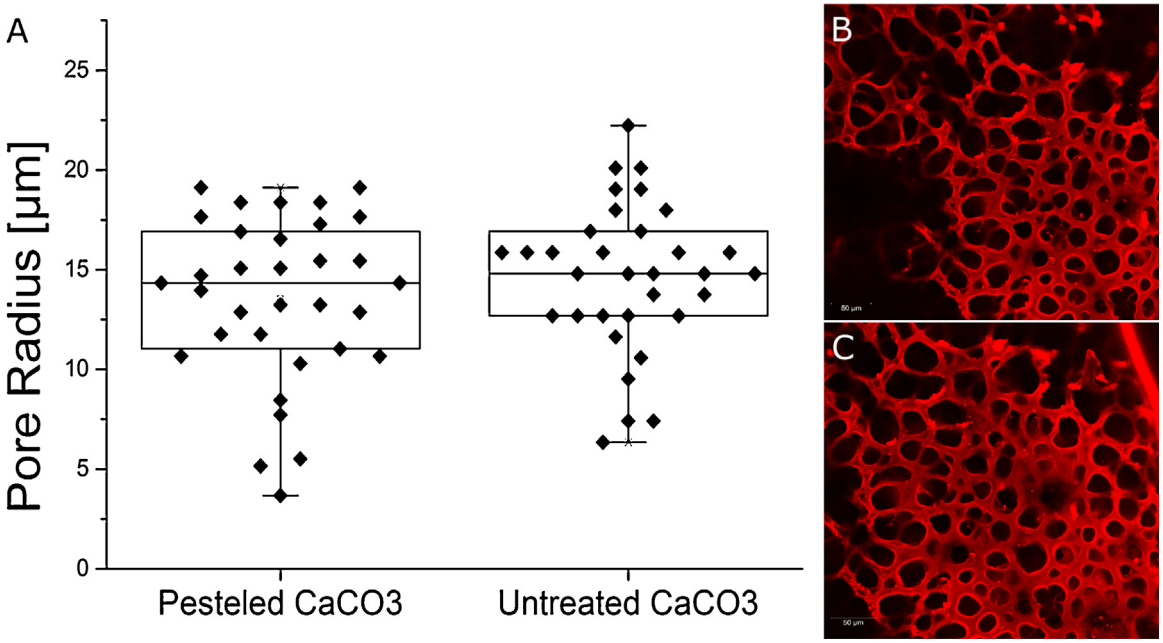

Fig. 4. Size and distribution of pores in protein hydrogels treated with a chalk-leaching procedure. (A) Size distribution of pores within the protein hydrogels matrix for hydrogels which were mixed with untreated $CaCO_3$ (B) and $CaCO_3$ which was grinded with a pestle and mortar for 10 min. (C). Hydrogels were stained with rhodamine B and investigated via confocal laser scanning microscopy. Scale bar 50 µm.

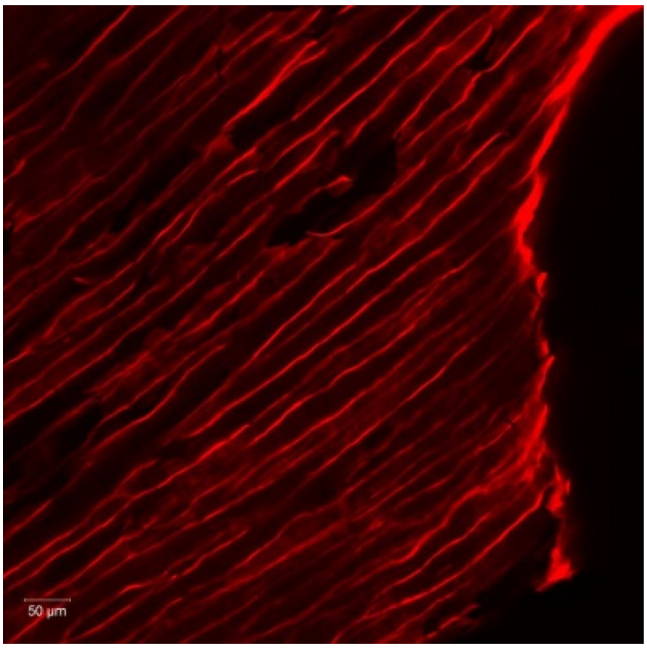

Fig. 5. Structure of protein hydrogel which was treated with a gradient freezing method: protein hydrogels were placed on a block of dried ice at 37 °C for 10 min, stained with rhodamine B in PBS for 30 min and visualized with confocal laser scanning microscopy at 514 nm. Scale bar 50 µm.

can be concluded that the very simple procedures described here are already sufficient for most applications in 3D cell culture as the radius of the resulting pores sizes can be tuned within the range of 10–80 µm (Figs. 2–4). Furthermore, these methods do not include any harmful or toxic components which remain in the network and might influence cell growth. Finally, a gradient freezing procedure was applied to form channels within hydrogels. Channel structures within a matrix have already been shown to facilitate the growth of axons in rats [23] and to enable linearly oriented nerve guidance with a mean pore radius of about 65 µm [25]. In this study, different setups with liquid nitrogen and dry ice were examined; hydrogels transferred into a puddle of liquid nitrogen showed fast evaporation effects and unequal freezing, resulting in a broken network with uneven pore distribution (data not shown). Best results were achieved when protein hydrogels were put onto a block of dried ice at 37 °C for about 10 min. High gradients in temperature lead to a gradual freezing of ice crystals, leading to channel formation in the gel with a pore radius of about 25 µm in average and a length of several hundreds of µm (Fig. 5). Those networks may be used for growth of specific cell types along the channels while the procedure is facile and does not require any special equipment.

Hydrogel resistance against temperature and pH is crucial for many features as hydrogels have to be stable under cell culture conditions for a prolonged time, have to be able to cope with harmful metabolic products, with acidic or basic conditions in the medium and with secreted proteolytic enzymes [21]. This is generally easy to fulfill for gels produced from non-natural or chemically synthesized compounds but often poses severe problems for protein hydrogels which are composed of a natural polymer and thus are often much weaker under these conditions [26]. Concerning thermal and pH resistance, particle leaching did not seem to have a tremendous influence on hydrogel properties as residual weight never fell below 90% for pH 2.0, 7.4, RT and 37 °C (Table 1). For basic conditions and high temperatures, a higher decrease in weight could be detected, whereas the type of technique does not seem to have any influence on stability, although less weight is lost than in untreated gels. To sum it up, none of the here presented methods seem to negatively influence the stability of the BSA material, making all methods useful for the manipulation of 3D structures for this protein based material.

Swelling ratio has to be taken into consideration as it is a good measurement for the free water within the matrix, which is crucial the use of hydrogels in 3D cell culture [27]. Here, swelling ratio varies between 534% and 1312% (Table 1) and values seem to correlate directly with the size of the pores. For hydrogels with pesteled NaCl crystals, the smallest pores and the lowest swelling ratio could be detected, whereas highest ratio was found for pores with biggest pore sizes. For cell culture application, a highly hydrated environment is desirable because it leads to better nutrition of cells, higher diffusion rates of supplements and fast removal of toxic metabolites [27]. On the other hand, pore size has to be in a good range to allow cell growth and infiltration. No matter which procedure was applied, water uptake was only influenced by pore size.

The degradability of hydrogels is often desirable for many applications but quite often difficult to realize for hydrogels made from artificial precursors. To overcome this problem, a protease sensitive BSA backbone was used as a cleavable component. Hydrogel degradation by enzymatic degradation is greatly accelerated upon pore size enlargement. A decreased degradation time is often required for hydrogel removal; networks should be destabilized to a breakdown point and eventually be completely removed [28]. It takes days to degrade tightly crosslinked hydrogels like the presented BSA-THPC hydrogels [17] as enzymes

Table 1
Influence of hydrogel preparation methods on hydrogel pH resistance, temperature resistance and swelling ratio measured after a period of 7 days at described conditions. Values represent the average residual weight [%] of hydrogels after 7 days.

Preparation Method	Residual weight at pH 2.0 [%]	Residual weight at pH 7.4 [%]	Residual weight at pH 10.0 [%]	Residual weight at RT [%]	Residual weight at 37 °C [%]	Residual weight at 80 °C [%]	Swelling ratio [%]
Grinded salt particles (10 min)[a]	96.2 ± 3.3	94.4 ± 4.2	86.1 ± 3.2	95.4 ± 0.42	97.4 ± 0.4	83.6 ± 4.5	534% ± 45%
Untreated salt particles	95.3 ± 3.8	95.6 ± 2.3	82.1 ± 4.4	97.4 ± 4.4	95.3 ± 4.2	81.2 ± 4.4	1153% ± 110%
Frozen at −20 °C	94.4 ± 3.4	95.3 ± 5.6	76.3 ± 5.5	91.3 ± 2.2	93.2 ± 3.3	84.2 ± 4.9	1312% ± 91%
Frozen in liquid nitrogen	96.2 ± 5.2	94.2 ± 3.2	83.2 ± 4.3	94.3 ± 4.1	96.2 ± 1.9	83.5 ± 3.4	834% ± 78%
$CaCO_3$ particles	94.2 ± 6.2	95.5 ± 3.2	82.3 ± 4.4	99.3 ± 5.5	96.5 ± 2.1	78.4 ± 1.3	746% ± 64%
Gradient freezing on dry ice	89.7 ± 4.3	94.1 ± 3.2	84.2 ± 4.5	97.1 ± 1.9	95.3 ± 4.3	91.4 ± 8.1	823% ± 163%
Untreated protein hydrogels	69.5 ± 4.4	98.2 ± 1.6	42.3 ± 4.1	99.1 ± 2.2	98.3 ± 3.4	70.2 ± 6.2	–

[a]NaCl crystals were grinded with a pestle and mortar for 10 min prior to use

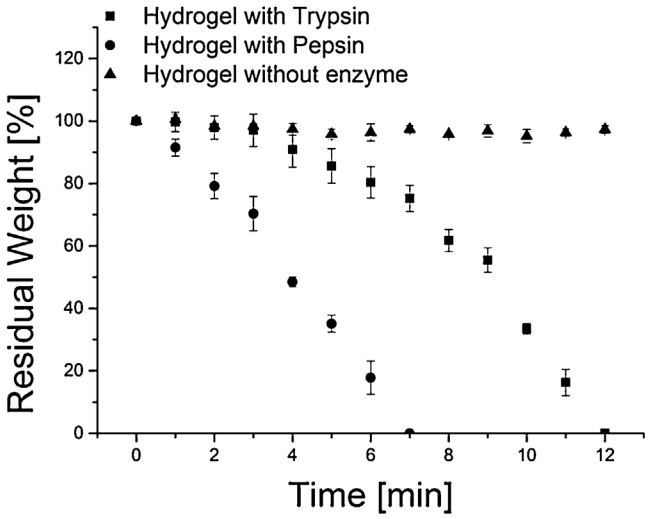

Fig. 6. Representative enzymatic degradation pattern for macroporous hydrogels treated with a particle leaching approach and incubated with 300 U of trypsin (pH 7.4) and pepsin (pH 2.0) over a period of 12 h.

have to work by diffusing and degrading from the outside to the inside of the network, thereby leading to minor changes in the beginning but causing a complete breakdown of 3D network after a certain time. As for gels with extended pore sizes, enzymes can cause proteolytic degradation at different location in the network at the same time, thus decreasing degradation time to several hours (Fig. 6). The temperature shift prior to drying – and the resulting increased pore size – further decreases the half-life of hydrogels from 2.4 h to 3.8 h for pepsin degradation and from 3.2 h up to 6.5 h for trypsin degradation respectively. A clear trend can be observed as pore sizes correlate with the degradation time, leading to a difference in half-life up to 17-fold (Table 2). As many hydrogels are designed for internal use, this has to be taken into consideration as proteolytic processes take place in large scale in the body.

In order to investigate the principal potential to use the presented macroporous materials in cell culture, the matrix was co-polymerized with a cell adhesive RGD peptide. A specific linker with a free primary amine was used to link the peptide during polymerization with the hydroxy groups of THPC and thus with the backbone of the gel. Human breast cancer cells and adenocarcinomic human alveolar basal epithelial cells were seeded onto the surface of a polymerized hydrogel and observed via laser scanning confocal imaging. For untreated hydrogels, no cell adhesion was detected whereas cells on functionalized hydrogels showed a strong adhesion onto the material (Fig. 7). This easy, single step co-polymerization of peptide to promote cell adhesion can be applied in both two dimensional as well as in three dimensional systems, making the produced hydrogel a versatile system for cell culture application.

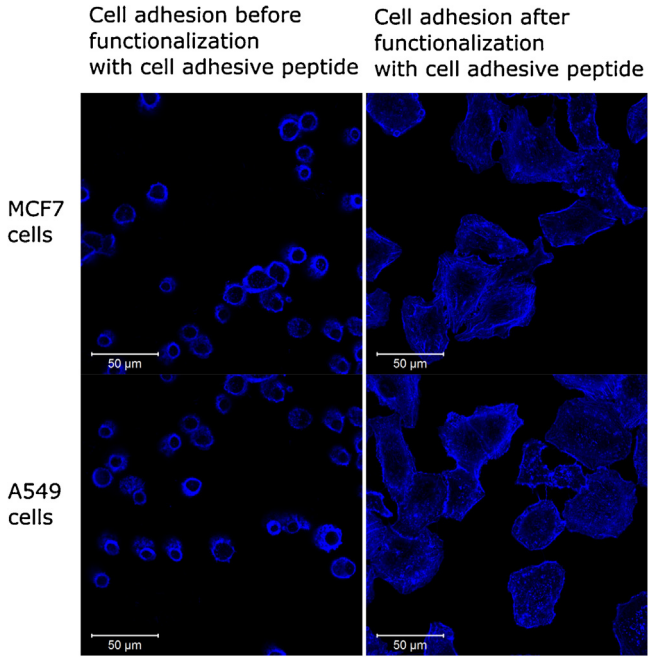

Fig. 7. Growth and adhesion of cells onto a functionalized protein hydrogel. $2*10^5$ cells were seeded onto a hydrogel surface on native (left side) and functionalized (right side) hydrogels. To functionalize hydrogels, a cell-adhesive RGD peptide was co-polymerized during hydrogel formation. After 24 h, the cells were stained with 5 µl of 300 U phalloidin-rhodamine B in 200 µl PBS and cellular adhesion of MCF7 and A549 cells was observed at 514 nm at a confocal laser scanning microscopy.

4. Conclusion

With the presented degradable protein hydrogel and some cheap and facile methods (particle leaching, freeze-drying and gradient freezing), hydrogel structures could be manipulate to form pores from 5 to 90 µm in radius and channels with a length up to several hundreds of µm and an average size of 25 µm radius, which covers most desired application for 3D cell culture [9,10,29]. Free water content within the matrix directly depends on pore size, and none of the procedures seemed to influence stability towards pH and temperature. Furthermore, hydrogels are enzymatically degradable due to the cleavable BSA backbone. Two different cell lines, A549 and MCF7 cancer cells lines showed a strong adhesion onto the material and were successfully grown on top of RGD functionalized hydrogels. We consider the developed material, especially because of the low costs and the simplicity to tune and modify hydrogels properties, to be a good option for initially evaluate 3D cell culture application while more sophisticated, high-tech approaches can still be put into effect for more specific questions.

Table 2
Influence of hydrogel preparation methods on enzymatic degradation pattern for trypsin and pepsin (300 U). Values represent half-life of hydrogels in solution [h].

	Half-life of pepsin-treated hydrogels [h]	Half-life of trypsin-treated hydrogels [h]
Pesteled salt particles (10 min)[a]	4.0 ± 0.21	7.4 ± 0.28
Untreated salt particles	3.1 ± 0.20	4.5 ± 0.23
Frozen at −20 °C	2.4 ± 0.14	3.2 ± 0.21
Frozen in liquid nitrogen	3.8 ± 0.17	6.5 ± 0.13
$CaCO_3$ particles	3.0 ± 0.24	4.0 ± 0.19
Gradient freezing in dry ice	3.5 ± 0.24	4.2 ± 0.19
Untreated protein hydrogels	46.5 ± 0.39	55.0 ± 0.31

[a] NaCl crystals were grinded with a pestle and mortar for 10 min prior to use.

N.B and F.R. thanks the “Baden-Württemberg Stiftung” for funding the work in the project in the framework “Bioinspired Materials Synthesis”.

References

[1] H. Park, X. Guo, J.S. Temenoff, Y. Tabata, A.I. Caplan, F.K. Kasper, A.G. Mikos, P.O. Box, Effect of swelling ratio of injectable hydrogel composites on chondrogenic differentiation of encapsulated rabbit marrow mesenchymal stem cells in vitro, Biomacromolecules 10 (2010) 541–546.

[2] A. Raic, L. Rödling, H. Kalbacher, C. Lee-Thedieck, Biomimetic macroporous PEG hydrogels as 3D scaffolds for the multiplication of human hematopoietic stem and progenitor cells, Biomaterials 35 (2014) 929–940.

[3] X.J. Li, A.V. Valadez, P. Zuo, Z. Nie, Microfluidic 3D cell culture: potential application for tissue-based bioassays, Bioanalysis 4 (2012) 1509–1525.

[4] J.-I. Sasaki, T.-A. Asoh, T. Matsumoto, H. Egusa, T. Sohmura, E. Alsberg, M. Akashi, H. Yatani, Fabrication of three-dimensional cell constructs using temperature-responsive hydrogel, Tissue Eng. Part A 16 (2010) 2497–2504.

[5] U.D. Hikmet Geckil Feng Xu Xiaohui Zhang SangJun Moon, Engineering hydrogels as extracellular matrix mimics, Nanomedicine 5 (2011) 469–484.

[6] K.E. Sung, X. Su, E. Berthier, C. Pehlke, A. Friedl, D.J. Beebe, Understanding the impact of 2D and 3D fibroblast cultures on in vitro breast cancer models, PLoS One 8 (2013) 1–13.

[7] G. Sun, X. Zhang, Y.-I. Shen, R. Sebastian, L.E. Dickinson, K. Fox-Talbot, M. Reinblatt, C. Steenbergen, J.W. Harmon, S. Gerecht, Dextran hydrogel scaffolds enhance angiogenic responses and promote complete skin regeneration during burn wound healing, Proc. Natl. Acad. Sci. U. S. A. 108 (2011) 20976–20981.

[8] J.A. Burdick, G. Vunjak-Novakovic, Engineered microenvironments for controlled stem cell differentiation, Tissue Eng. Part A 15 (2009) 205–219.

[9] K. Whang, K.E. Healy, D.R. Elenz, E.K. Nam, D.C. Tsai, C.H. Thomas, G.W. Nuber, F. H. Glorieux, R. Travers, S.M. Sprague, Engineering bone regeneration with bioabsorbable scaffolds with novel microarchitecture, Tissue Eng. 5 (1999) 35–51.

[10] I.V. Yannas, E. Lee, D.P. Orgill, E.M. Skrabut, G.F. Murphy, Synthesis and characterization of a model extracellular matrix that induces partial regeneration of adult mammalian skin, Proc. Natl. Acad. Sci. U. S. A. 86 (1989) 933–937.

[11] Volodymyr Samaryk, Andriy Voronov, Ihor Tarnavchyk, Ananiy Kohut, Natalya Nosova, Serhiy Varvarenko, Stanislav Voronov, A versatile approach to develop porous hydrogels with a regular pore distribution and investigation of their physicomechanical properties, J. Appl. Polym. Sci. 114 (2009) 2204–2212.

[12] S. Agarwal, J.H. Wendorff, A. Greiner, Use of electrospinning technique for biomedical applications, Polymer (Guildf.) 49 (2008) 5603–5621.

[13] J. Hong, A.J. deMello, S.N. Jayasinghe, Bio-electrospraying and droplet-based microfluidics: control of cell numbers within living residues, Biomed. Mater. 5 (2010) 21001.

[14] J. Lee, M.J. Cuddihy, N.A. Kotov, Three-dimensional cell culture matrices: state of the art, Tissue Eng. Part B Rev. 14 (2008) 61–86.

[15] Y.-C. Chiu, S. Kocagöz, J.C. Larson, E.M. Brey, Evaluation of physical and mechanical properties of porous poly (ethylene glycol)-co-(L-lactic acid) hydrogels during degradation, PLoS One 8 (2013) e60728.

[16] J. He, Rapid generation of biologically relevant hydrogels containing long-range chemical gradients, Adv. Funct. Matter 20 (2010) 131–137.

[17] N. Bodenberger, P. Paul, D. Kubiczek, P. Walther, K. Gottschalk, F. Rosenau, A novel cheap and easy to handle protein hydrogel for 3D cell culture applications: a high stability matrix with tunable elasticity and cell adhesion properties, Chem. Sel. 1 (2016) 1353–1360.

[18] E. Calo, V.V. Khutoryanskiy, Biomedical applications of hydrogels: a review of patents and commercial products, Eur. Polym. J. 65 (2015) 252–267.

[19] R.P. Ramasamy, C. Gordon, P. Brink, A novel soluble hydrogel cell culture bioreactor made using proteins, Adv. Porous Mater. 3 (2015) 40–45.

[20] L.S. Moreira Teixeira, J. Feijen, C.A. van Blitterswijk, P.J. Dijkstra, M. Karperien, Enzyme-catalyzed crosslinkable hydrogels: emerging strategies for tissue engineering, Biomaterials 33 (2012) 1281–1290.

[21] M.S. Shoichet, R.H. Li, M.L. White, S.R. Winn, Stability of hydrogels used in cell encapsulation: an in vitro comparison of alginate and agarose, Biotechnol. Bioeng. 50 (1996) 374–381.

[22] P. Walther, Recent progress in freeze-fracturing of high-pressure frozen samples, J. Microsc. (2003) 34–43.

[23] E.C. Tsai, P.D. Dalton, M.S. Shoichet, C.H. Tator, Synthetic hydrogel guidance channels facilitate regeneration of adult rat brainstem motor axons after complete spinal cord transection, J. Neurotrauma 21 (2004) 789–804.

[24] J.J. Klawitter, S.F. Hulbert, Application of porous ceramics for the attachment of load bearing internal orthopedic applications, J. Biomed. Mater. Res. 5 (1971) 161–229.

[25] S. Stokols, M.H. Tuszynski, The fabrication and characterization of linearly oriented nerve guidance scaffolds for spinal cord injury, Biomaterials 25 (2004) 5839–5846.

[26] M. Ramirez, D. Guan, V. Ugaz, Z. Chen, Intein-triggered artificial protein hydrogels that support the immobilization of bioactive proteins, J. Am. Chem. Soc. 135 (2013) 5290–5293.

[27] J. Zhu, R.E. Marchant, Design properties of hydrogel tissue-engineering scaffolds, Expert Rev. Med. Devices 8 (2011) 607–626.

[28] G.D. Nicodemus, S.J. Bryant, Cell encapsulation in biodegradable hydrogels for tissue engineering applications, Tissue Eng. Part B Rev. 14 (2008) 149–165.

[29] N. Annabi, J.W. Nichol, X. Zhong, C. Ji, S. Koshy, A. Khademhosseini, F. Dehghani, Controlling the porosity and microarchitecture of hydrogels for tissue engineering, Tissue Eng. Part B Rev. 16 (2010) 371–383.